

Size dependence of dynamic fluctuations in liquid and supercooled water

Cite as: J. Chem. Phys. **150**, 144505 (2019); <https://doi.org/10.1063/1.5085886>

Submitted: 16 December 2018 . Accepted: 14 March 2019 . Published Online: 09 April 2019

Joan Manuel Montes de Oca , Sebastián R. Accordino, Gustavo A. Appignanesi , Philip H. Handle, and Francesco Sciortino 



View Online



Export Citation



CrossMark

The Journal
of Chemical Physics

2018 EDITORS' CHOICE

READ NOW!



Size dependence of dynamic fluctuations in liquid and supercooled water

Cite as: J. Chem. Phys. 150, 144505 (2019); doi: 10.1063/1.5085886

Submitted: 16 December 2018 • Accepted: 14 March 2019 •

Published Online: 9 April 2019



View Online



Export Citation



CrossMark

Joan Manuel Montes de Oca,¹  Sebastián R. Accordino,¹ Gustavo A. Appignanesi,¹ 
Philip H. Handle,² and Francesco Sciortino^{3,4} 

AFFILIATIONS

¹INQUISUR, Departamento de Química, Universidad Nacional del Sur (UNS)-CONICET, Avenida Alem 1253, 8000 Bahía Blanca, Argentina

²Department of Physical Chemistry, University of Innsbruck, Innrain 52c, A-6020 Innsbruck, Austria

³Dipartimento di Fisica, Sapienza Università di Roma, Piazzale A. Moro 5, Roma 00185, Italy

⁴CNR-ISC, c/o Sapienza, Piazzale A. Moro 5, Roma 00185, Italy

Note: This paper is part of a JCP Special Topic on Chemical Physics of Supercooled Water.

ABSTRACT

We study the evolution of dynamic fluctuations averaged over different space lengths and time scales to characterize spatially and temporally heterogeneous behavior of TIP4P/2005 water in liquid and supercooled states. Analyzing a 250 000 molecules simulated system, we provide evidence of the existence, upon supercooling, of a significant enhancement of spatially localized dynamic fluctuations stemming from regions of correlated mobile molecules. We show that both the magnitude of the departure from the value expected for the system-size dependence of an uncorrelated system and the system size at which such a trivial regime is finally recovered clearly increase upon supercooling. This provides a means to estimate an upper limit to the maximum length scale of influence of the regions of correlated mobile molecules. Notably, such an upper limit grows two orders of magnitude on cooling, reaching a value corresponding to a few thousand molecules at the lowest investigated temperature.

Published under license by AIP Publishing. <https://doi.org/10.1063/1.5085886>

I. INTRODUCTION

When we cool a liquid fast enough to prevent crystallization, we obtain a supercooled liquid that ultimately transforms into a glass, a solid metastable material with disordered liquid-like structure.^{1,2} However, even if from a practical point of view, this process has been known for centuries; the comprehension of the molecular expedient by which the liquid falls out of equilibrium remains one of the most interesting topics in condensed matter physics.^{3–9} A major breakthrough was the discovery of dynamical heterogeneities, regions of atoms or molecules moving in a cooperative way, in a spatially and temporally heterogeneous fashion.^{10–14} At any particular time, certain regions of the sample are virtually frozen, while others are quite mobile and characterized by a “cooperative” motion where localized groups of molecules exhibit significant displacements.^{12,15–17} While early studies^{15–17} used somewhat arbitrary criteria to define mobile particles, later studies examined

spatial correlation functions averaged over all particles in various ways attempting to identify the length and time scales of dynamical heterogeneity.^{12,17–28} Particularly useful insights have resulted from four-point correlation functions such as the four-point dynamical susceptibility, χ_4 (see Ref. 29 for a comprehensive review).

Slow dynamics in liquid water has also received significant attention. Water is central for many fields ranging from biology to materials science.^{30–43} Within such contexts, being usually at interfaces or subject to nanoconfinement, water usually shows certain reminiscences of glassy behavior even at room temperature.^{34–41} Indeed, pure supercooled water represents a system of huge interest in itself since it exhibits an unusual behavior whose comprehension still remains incomplete despite intense experimental and theoretical studies on both thermodynamical and dynamical grounds.^{44–67} Computationally, it has been shown that dynamical heterogeneities are also observed in supercooled water, with mobile

molecules arranged in clusters that perform collective relaxing motions.^{72,73}

Recently, some of us have introduced a new approach to characterize spatial and temporal dynamical heterogeneity that does not require any *a priori* definition of particle mobility. This has been achieved by using a parameter-free method (that is, without employing any mobility threshold or classifying molecules as mobile) that contrasts spatial and temporal motion within regions of a system with corresponding quantities evaluated in the large system limit and averaged over space and time.⁷⁴ Specifically, we used the system average mean square displacement (MSD) as a “null hypothesis” for particle motion and we quantified deviations away from this null hypothesis by focusing on the system’s localized dynamic fluctuations, employing a block-analysis method similar to previous approaches used within the context of the four-point susceptibility (χ_4) function.^{75,76} In Ref. 74, we applied this method to two archetypal glass-forming systems: computer simulations of the Kob-Andersen mixture⁷⁷ and confocal microscopy data of colloidal suspensions.⁷⁸ For thermodynamic conditions for which motion is homogeneous in space and time (i.e., particle motion is not significantly correlated), we corroborated the expected behavior that the normalized dynamic fluctuations scale with a $N^{-1/2}$ power law decay. However, as the relaxation enters the glassy regime, the appearance of regions of correlated mobile particles makes the spatially localized dynamic fluctuations depart from such trivial behavior, decaying much slower with system size. In this work, we apply the same methodology to computer simulations of liquid water. By a careful study of the size-dependence of the molecular dynamic fluctuations, we show the existence of an initial power law decay (that gets progressively slower as we supercool the system) before the trivial system-size dependence is recovered at large N . The crossover to the $N^{-1/2}$ regime provides an upper limit to the size of the largest spatially correlated relaxing regions. Additionally, we demonstrate that this regime is approached at larger N values as temperature T decreases, suggesting a clear increase in the length scale of spatial heterogeneity on supercooling.

II. SIMULATION DETAILS

We perform NVT simulations using the TIP4P/2005⁷⁹ model of water, which has emerged as the present-day optimal rigid water model.⁸⁰ All simulations are conducted utilizing GROMACS 5.1.4⁸¹ with a velocity-Verlet integrator using a time step of 1 fs. The temperature is controlled using a Nosé-Hoover thermostat^{82,83} while the Coulombic interactions are evaluated using a particle mesh Ewald treatment⁸⁴ with a Fourier spacing of 0.1 nm^{-1} . The bond constraints are maintained using the LINCS (Linear Constraint Solver) algorithm.⁸⁵ For both the Lennard-Jones and the real space Coulomb interactions, an identical cutoff $r_{\text{cut}} = 0.9 \text{ nm}$ is used. Lennard-Jones interactions beyond r_{cut} have been included, assuming a uniform fluid density. The TIP4P/2005 system consists of $N_{\text{max}} = 250\,000$ molecules in a cubic box at density 0.95 g/cm^3 and it was studied at several T , ranging from 230 to 360 K. We have chosen to investigate the $\rho = 0.95 \text{ g/cm}^3$ isochore to avoid interference of the dynamics from the possible presence of a liquid-liquid critical point, predicted to be above the $\rho = 1.00 \text{ g/cm}^3$ isochore.^{66,68–71}

III. RESULTS

The starting point of the method is the observation of dynamic intermittency in molecular motion.⁷⁴ Following prior studies,^{23–27,73,74,86} we compute a distance matrix $\Delta_S^2(t', t'')$, which represents the average of the squared molecular displacements between times t' and t'' of a collection of N water molecules belonging to a predefined set S (S may be the entire system or a subsystem, a subvolume of the simulated system)

$$\Delta_S^2(t', t'') \equiv \frac{1}{N} \sum_{i=1}^N |\vec{r}_i(t') - \vec{r}_i(t'')|^2 \quad (1)$$

$$= \langle |\vec{r}_i(t') - \vec{r}_i(t'')|^2 \rangle_{i \in S}, \quad (2)$$

where the sum in Eq. (1) runs over the N particles i belonging to S and the angle brackets in Eq. (2) indicate an average over only these N molecules. Further averaging $\Delta_S^2(t', t'')$ over all pairs t' and t'' such that $t'' - t' = \Delta t$ yields the well-known average mean square displacement $MSD(\Delta t)$ of the molecules in S . More precisely, $MSD(\Delta t) = \langle \Delta_S^2(t', t'') \rangle_{t''-t'=\Delta t}$, where the average is over t' , t'' with fixed time interval $\Delta t = |t'' - t'|$ and also over all of the particles in S . Under stationary dynamics and for a sufficiently large Δt , $\lim_{\Delta t \rightarrow \infty} \Delta_S^2(t', t' + \Delta t) = MSD(\Delta t)$.

For small systems under glassy relaxation conditions, Δ_S^2 has temporal fluctuations, as shown in Fig. 1(a) for a subsystem S corresponding to $N = 250$ water molecules at $T = 230 \text{ K}$. Darker regions indicate the existence of time intervals (t' , t'') over which this subsystem has relatively little particle motion to then undergo rapid bursts of mobility. The latter events have been shown to involve the correlated large displacement of a relatively compact cluster of molecules that drive the system from one metabasin of its potential energy surface to a neighboring one.^{23–27,73,74} On a mechanistic basis, these collective motions could be related to coupled translational and rotational jumps⁸⁷ found in a single-molecule trajectory analysis⁸⁸ and to similar events found by Fabbian *et al.*⁸⁹ However, further work would be demanded in order to establish a clear quantitative link. Since different regions within a large sample would suffer these relaxing events at different times, the island structure of the distance matrix begins to be washed out as we increase the size of the subsystem under study²⁴ (the spatial fluctuations average out such that $\lim_{N \rightarrow \infty} \Delta_S^2(t', t' + \Delta t) = MSD(\Delta t)$). In other words, on increasing the subsystem size well beyond any dynamic correlation length, the independent behavior of the different regions of the system that are located sufficiently far apart⁷² make Δ_S^2 to appear much smoother at any given time, as shown in Fig. 1(b) for the entire system. In turn, as T is decreased, it is expected that the sizes of the correlated relaxing regions increase, and thus, we have to go to larger subsystem sizes in order to get a smooth distance matrix.

In a similar fashion as done for studies based on block-analysis of the four-point susceptibility (χ_4),^{75,76} we focus on the way in which the large system limit is reached and how this relates to the spatial scale of dynamical heterogeneities.⁷⁴ Since the obvious features of Fig. 1(a) are the large fluctuations that differentiate it from Fig. 1(b), we consider the normalized difference between Δ_S^2 and the expectation for a large system,⁷⁴ defined by

$$\Omega_S^2(t', t'') = \frac{[\Delta_S^2(t', t'') - MSD(\Delta t)]^2}{[MSD(\Delta t)]^2}, \quad (3)$$

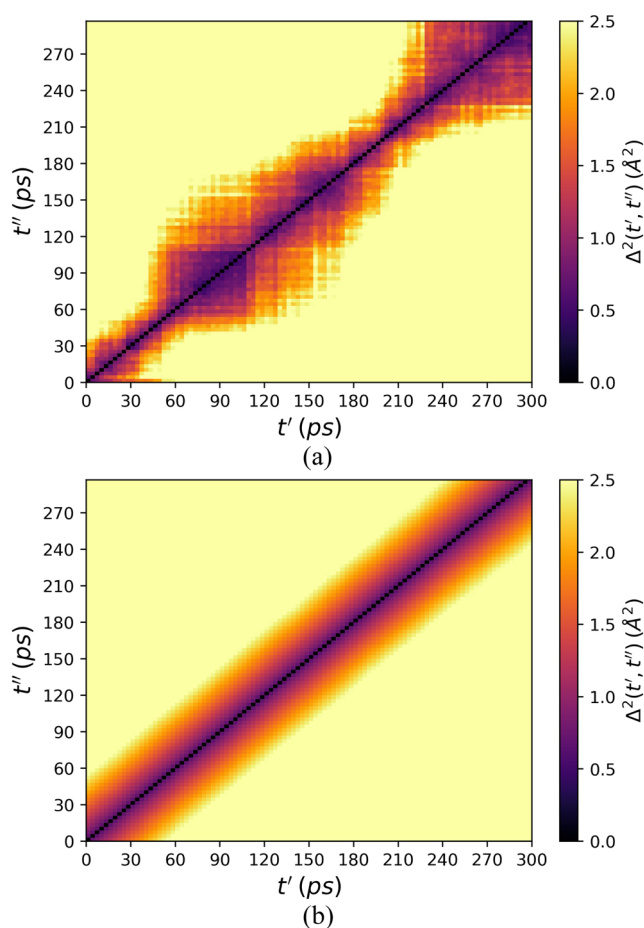


FIG. 1. (a) Contour plot of the distance matrix $\Delta_S^2(t', t'')$ for a TIP4P/2005 water cubic subsystem S represented by a compact cubic block containing $N = 250$ molecules extracted from the simulated $N_{\max} = 250\,000$ system at $T = 230$ K. (b) Contour plot of the same system for the full $N_{\max} = 250\,000$ molecules simulation.

with the convention $\Delta t = |t'' - t'|$. Ω_S^2 represents the matrix of normalized squared deviations from the mean value for the squared displacements of the water molecules and will be equal to zero when Δ_S^2 is calculated for sufficiently large systems, for which time averages and space averages are equivalent and $\Delta_S^2 = MSD$. Otherwise, $\Omega_S^2 > 0$ and larger values indicate larger deviations between Δ^2 (local in both space and time) and the expectation for a large system (that is, MSD , a quantity averaged over all space and all time). Thus, $\Omega_S^2(t', t'')$ provides us with a measure of dynamic intermittency. In simple terms, it reflects how different is the distance matrix for a small subsystem of size N at a given time [similar to Fig. 1(a)] from the situation when the results are averaged in size (large system) or, equivalently, in time [an outcome consistent with that shown in Fig. 1(b)]. In practice, for each subsystem of interest, we calculate $\Omega_S^2(t', t'')$ for all the matrix elements of its distance matrix [at low temperature, the distance matrix for any of such subsystems would look like Fig. 1(a) if the subsystems are small enough]. For time intervals when we are within an island [as the ones depicted

in Fig. 1(a)], the relaxation is virtually stuck, and thus, the measure reflects the deviation of the relaxation behavior of the subsystem from the corresponding expected value for the large system (that is, MSD , the mean squared displacement value corresponding to such time interval). In turn, when we focus on time intervals framing an island transition, like that depicted in Fig. 1(a), we are faced with a large burst of mobility that also deviates from the more modest value corresponding to MSD for such time interval. Thus, in the calculation of the Ω_S^2 function, we compute squared deviations in order to sum up both the excess and defect contributions that originate from all time intervals or matrix elements. Additionally, we make the calculation relative to MSD in order to be left with normalized dynamic fluctuations.

It is noteworthy that the Ω_S^2 function is local both in space and time. To focus on the spatial dependence of the fluctuations, we need to integrate out the time dependence. To do so, we calculate the ratio of the dispersion to the average⁹⁰ for the molecular squared displacements. We partition the large system of $N_{\max} = 250\,000$ molecules into distinct cubical boxes (blocks) containing N molecules each. For each box, we evaluate the sum of $\Omega_S^2(t', t'')$ over all time pairs (t', t'') divided by the total number of such pairs. We then average the resulting number over all boxes and finally take the square root of the result. Repeating this procedure for several N values yields the desired time-independent quantity $\Omega(N)$. Note that we define the N molecules in a box at an initial time and then we study their behavior in time. While some molecules might leave the original box during their trajectories, we note that this is not significant since the total time for the evaluation of the $\Omega(N)$ function corresponds to the time scale when the molecules have moved on average only one inter-particle distance.

As noted in a prior work,⁷⁴ the magnitude of $\Omega(N)$ depends on the total time studied, that is, the maximum of $|t'' - t'|$ that is included in the calculation. Large $|t'' - t'|$ time intervals contribute with small values and, thus, decrease $\Omega(N)$.⁷⁴ However, for a given dataset, the magnitude of the function is not relevant since the N -dependence is insensitive to the total time studied, provided that such time is able to capture the temporal fluctuations present in the distance matrix.⁷⁴ In other words, what matters is to include a few of the “islands” seen in Fig. 1(a).⁷⁴ Consistently, in this work, we adopt a time scale that represents a good choice in order to render a satisfactory $\Omega(N)$ function for the data we have examined. We thus take a total time given by the time scale when, at each temperature, the MSD equals the (squared) nearest neighbor distance (the first peak position in the O–O radial distribution function), that is, the time when all the water molecules in the system have on average moved one intermolecular distance. This value, which is not far from the time scale of the maximum in the time dependence of the non-gaussian parameter and of the α -relaxation time, lies after the plateau of the mean squared displacement curve (just beyond the end of the caging regime), at the beginning of the diffusive regime. At such time, all the molecules have been able, on average, to break their first neighbors confinement in order to perform a significant local relaxation event.

Figure 2 displays the function $\Omega(N)$ for TIP4P/2005 water at temperatures $T = 230, 240, 250, 270, 300, 330,$ and 360 K. Similar to the simulations of the Kob-Andersen binary Lennard-Jones mixture and the experiments on colloidal suspensions we studied

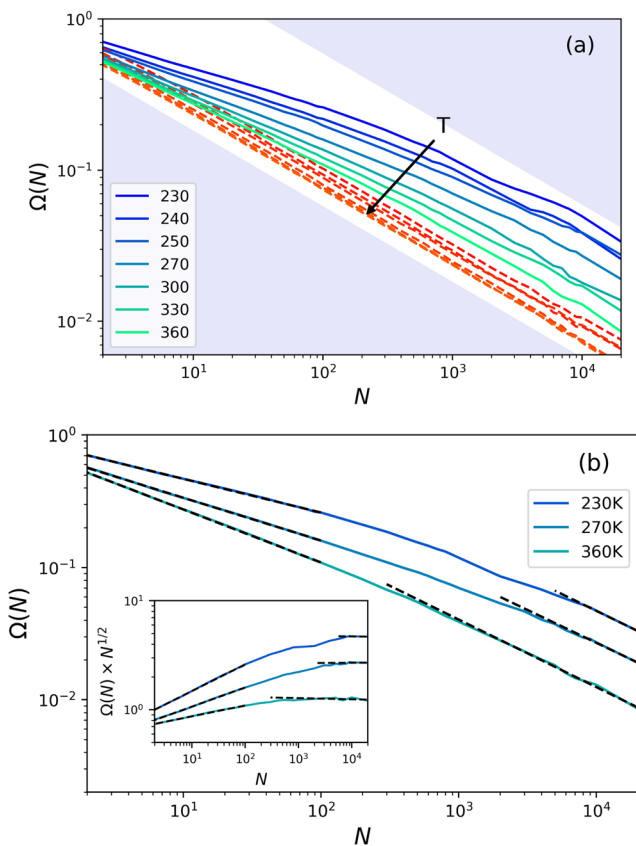


FIG. 2. (a) $\Omega(N)$ (blue and green lines) and $\Omega_R(N)$ (red dotted lines) as a function of subsystem size N for TIP4P/2005 for different temperatures as indicated (the arrow indicates the way of increase in temperature for both cases). In the case of $\Omega(N)$, the N molecules are part of the same compact subsystem (cubical block). In the case of $\Omega_R(N)$, the N particles are selected *randomly* among all the molecules in the system. The size of the simulated system is always $N_{\max} = 250\,000$. We do not plot data for N larger than $N = N_{\max}/10$, as we need to average over at least 10 subsystems in order to get enough statistics to evaluate a reasonable. The shaded regions are provided as a means to help guide the eye towards identification of slopes $-1/2$. (b) Same data as in (a) for $T = 230, 270,$ and 360 K displaying the two relevant regimes: The first one with a decay that gets progressively slower as T decreases and a last regime consistent with the trivial $N^{-1/2}$ size-dependence of the fluctuations. The latter regime is approached at higher N as T is lowered. Both regimes are fitted by the dotted lines, as indicated in the text. The inset shows the same data but multiplying $\Omega(N)$ by the function $N^{1/2}$. This would be similar to dividing $\Omega(N)$ by $\Omega_R(N)$.⁷⁴

before,⁷⁴ the dynamical fluctuations average out for large subsystem sizes. On cooling, larger and larger subsystems are required before the dynamical fluctuations are averaged out. We also included in Fig. 2 the function $\Omega_R(N)$ computed using N randomly chosen particles within the simulated system, destroying by construction any correlation in the motion of nearby particles (the subscript R stresses the random choice). Direct inspection of Fig. 2 shows that for these curves, the heterogeneity is quickly averaged out with N , following a power law whose exponent does not depend on T .

The functional form of the decay of $\Omega(N)$ with N provides the most relevant piece of information.⁷⁴ Figure 2 shows that the

randomly distributed dynamical fluctuations quantified by $\Omega_R(N)$ display a trivial system-size dependence, that is, they yield the typical $N^{-1/2}$ decay at all temperatures. This reflects that particle motion is nearly spatially uncorrelated within a subsystem and so the average of $\Delta_S^2(N)$ converges to the large-system limit MSD as $N^{-1/2}$. In turn, when $\Omega(N)$ is evaluated within compact subsystems of size N , we get a completely different picture. In a similar fashion as obtained for the Lennard-Jones mixture and for the experimental data on colloidal suspensions,⁷⁴ a clear departure from this trivial behavior is observed as the temperature is decreased since the decay of $\Omega(N)$ gets progressively slower. This significant enhancement of the spatially localized dynamical fluctuations, persisting at large system sizes, reflects the existence of regions of correlated mobile particles, an effect that is more pronounced upon supercooling.^{12,15–17,20,78} As the temperature increases, we observe from Fig. 2 that the spatially localized dynamic fluctuations display a size scaling dependence progressively closer to the usual $N^{-1/2}$ scaling law.

At any given T , it is expected that the system presents a whole distribution of sizes of regions of correlated mobile particles. Provided we are working above the mode coupling temperature ($T_C = 204.6$ K at the density we are performing the simulations, $\rho = 0.95$ g/cm³, while it is $T_C = 191.5$ K at $\rho = 1.00$ g/cm³), the size of such regions are, in turn, expected to increase with the degree of supercooling. As already discussed above, if we consider small subsystems within a large system, these regions of correlated mobile particles would govern the relaxation, and thus, the deviations from the large-system expectation value would be significant. However, as we focus on subsystems of progressively larger sizes, larger than the typical sizes of the regions of correlated mobile particles (that is, when the collectively relaxing regions are small as compared to the blocks), we expect that this behavior begins to be averaged out until the decay reverts to the trivial scaling down. A careful study of subsystems within a large total system would, thus, enable us to quantify the way in which such a transition to the trivial regime occurs at a larger subsystem size, N , as the temperature is decreased. Thus, in Fig. 2(b), we plot again the function $\Omega(N)$ (that is, for the block analysis) for temperatures $T = 230, 270,$ and 360 K. From Fig. 2(b), it is immediately evident that the curves indeed present two clearly different regimes: a first power-law regime for the low N region where the relaxation is dominated by the spatially localized dynamic fluctuations arising from the collective motions, while at large N , the curves revert to the trivial system-size scaling (power law exponent of $-1/2$). The latter regime is indeed approached at larger N values as T decreases.

In Fig. 3, we plot the decay exponent [defined as the slope m from the logarithmic plot of Fig. 2(a)] of the first (small N) regime of $\Omega(N)$ as a function of T (the fit is performed in all cases up to $N = 100$, as depicted by the fitting lines in the figure). For the lowest T , $T = 230$ K, $m \approx -0.25$, depicting the reluctance of the dynamic fluctuations to fall with increasing size. This value decreases towards the trivial decay ($m = -0.5$) as T is incremented (for the largest T studied, $T = 360$ K, m is around -0.4). It is interesting to consider the results for TIP4P/2005 as compared to our former study of the Kob-Andersen binary Lennard-Jones mixture.⁷⁴ This is illustrated by the inset of Fig. 3, where we plot the data in units of the mode coupling temperature, T_C . First of all, we can note that the behavior of TIP4P/2005 water parallels nicely that of such an archetypal glass-former. Additionally, for $T = 360$ K for TIP4P/2005, we can

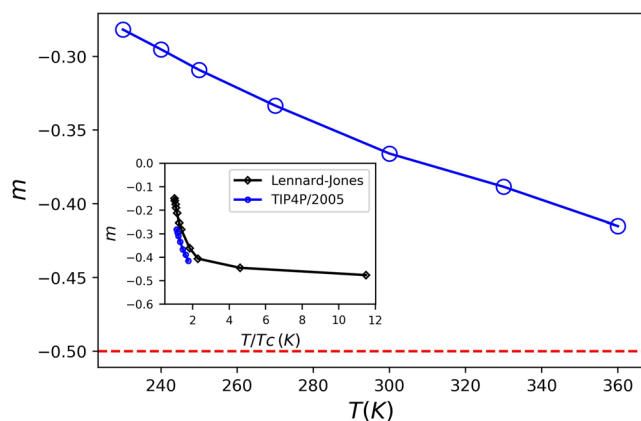


FIG. 3. Decay exponent for the low N regime of $\Omega(N)$ [slopes m from the logarithmic plots of Fig. 2(a)] as a function of temperature. The dashed line indicates trivial system-size scaling. In turn, the inset shows the same data but as a function of T/T_c , where T_c is the mode coupling temperature, and compares to the situation for the Kob-Andersen binary Lennard-Jones mixture studied in our previous work.⁷⁴

see that we are at $1.76T_c$, a situation which would correspond to a case slightly below $T = 1$ for the binary Lennard-Jones system. At this temperature, the latter has been shown to present a crossover from a “landscape influenced” glassy regime to a diffusive regime typical of larger temperatures lacking glassy behavior.⁹² Thus, it is expected that at $T = 360$ K for $\rho = 0.95$ g/cm³, the TIP4P/2005 system is close to the simple liquid diffusive regime but still presents certain spatial correlations that avoid it to reach the trivial regime at low N .

In turn, as already indicated, the N value where $\Omega(N)$ crosses to the trivial $N^{-1/2}$ decay indicates that the large-limit behavior has been reached. Such a crossover implies that the subsystem is now composed by a sufficiently large number of independently relaxing regions and, thus, represents the length scale at which the influence of the collective relaxation regions is averaged out. Qualitatively, direct inspection of Fig. 2(b) makes it clear that this happens at a much higher N as the temperature is lowered. To quantitatively estimate this length scale, we now study in detail the large N decay of $\Omega(N)$ (to avoid possible statistical errors, we consider the $\Omega(N)$ function at up to $N = N_{\max}/10$ to get at least 10 subsystems to evaluate a reasonable value). Starting at $N = N_{\max}/10$, we extend the theoretical decay regime to lower N values by imposing a -0.5 exponent (that is, a -0.5 slope in the logarithmic plot of $\Omega(N)$ vs N), provided the correlation coefficient is larger than 0.99. We then calculate the value of N for which $\Omega(N)$ deviates more than 3σ from this behavior, which marks the point of departure from the trivial regime as N is decreased. Figure 4 displays the results. The approach to the trivial size decay of the fluctuations, and thus, the length scale of maximal influence of the regions of correlated collective relaxation indeed depends strongly on temperature. Specifically, we find that for the lowest temperature studied, $T = 230$ K, it occurs at around $N = 5000$, a size almost two orders of magnitude larger than the situation for $T = 360$ K. These values are too large as compared to correlation lengths reported previously both experimentally⁹³ and

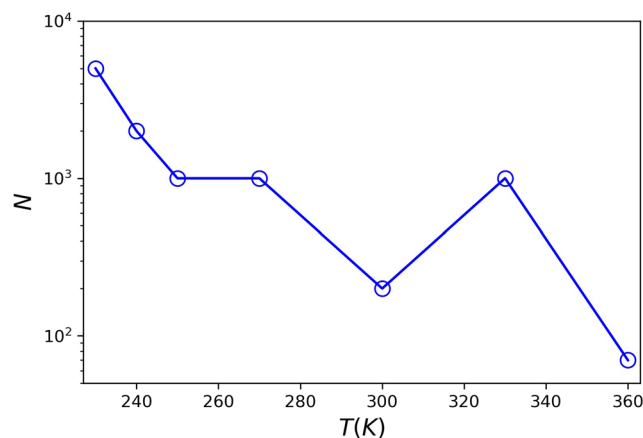


FIG. 4. Estimation of the length scale of approaching to the trivial $N^{-1/2}$ scaling regime for the different temperatures studied.

computationally.⁹⁴ We note that we just provide an upper limit to the maximum length scale of influence of the (much smaller) regions of correlated mobile molecules, that is, the scale necessary to average out their effect. In terms of the distance matrix representation of Fig. 1, it is the size at which the island structure disappears and the system completely stops “feeling” any effect from the correlations. However, what really matters is the dependence of this quantity with the temperature and not its absolute value. In turn, we also note that we have deliberately avoided to investigate an isochore that could end up close to the expected location of the critical point of TIP4P/2005. In future work, it could be interesting to repeat this analysis in the critical point region to investigate how spatial and dynamic correlations originating from the slowing down of the dynamics under supercooling behave when coupled to critical fluctuations.

IV. CONCLUSIONS

In this work, we have applied a measure of spatial and temporal dynamic heterogeneity to liquid and supercooled water by studying the evolution of dynamic fluctuations averaged over different space lengths and time scales. We have corroborated previous results in other glassy systems indicating that the appearance, upon supercooling, of regions of correlated mobile molecules makes the system present significant spatially localized dynamic fluctuations. A careful study of the size dependence of such dynamic fluctuations has now enabled us to distinguish two clearly different regimes: An initial regime in which fluctuations decay unusually slowly with system size, a behavior that is more conspicuous as the temperature is decreased while, at large length scales, the behavior recovers the trivial scaling down of dynamic fluctuations characterized by the typical $N^{-1/2}$ power law decay. The system size at which this final regime is approached significantly grows as T decreases, reaching values 100 times larger (in N) than the high- T limit. At the lowest temperatures studied, averaging out the influence of the regions of correlated mobile molecules requires approximately one thousand particles.

ACKNOWLEDGMENTS

G.A.A., S.R.A., and J.M.M.O. acknowledge support from CON-ICET, UNS, and ANPCyT (Grant No. PICT2015/1893). P.H.H. acknowledges support from the Austrian Science Fund (FWF Erwin Schrödinger Fellowship J3811 N34).

REFERENCES

- C. A. Angell, *Science* **267**, 1924 (1995).
- C. A. Angell, K. L. Ngai, G. B. McKenna, P. F. McMillan, and S. W. Martin, *J. Appl. Phys.* **88**, 3113 (2000).
- J. S. Langer, *Rep. Prog. Phys.* **77**, 042501 (2014).
- D. Chandler and J. P. Garrahan, *Annu. Rev. Phys. Chem.* **61**, 191 (2010).
- G. Biroli and J. P. Garrahan, *J. Chem. Phys.* **138**, 12A301 (2013).
- M. D. Ediger and P. Harrowell, *J. Chem. Phys.* **137**, 080901 (2012).
- V. Lubchenko and P. G. Wolynes, *Annu. Rev. Phys. Chem.* **58**, 235 (2007).
- A. Cavagna, *Phys. Rep.* **476**, 51 (2009).
- P. Charbonneau, J. Kurchan, G. Parisi, P. Urbani, and F. Zamponi, *Annu. Rev. Condens. Matter Phys.* **8**, 265 (2017).
- H. Sillescu, *J. Non-Cryst. Solids* **243**, 81 (1999).
- M. D. Ediger, *Annu. Rev. Phys. Chem.* **51**, 99 (2000).
- S. C. Glotzer, "Physics of non-crystalline solids 9," *J. Non-Cryst. Solids* **274**, 342 (2000).
- E. Hempel, G. Hempel, A. Hensel, C. Schick, and E. Donth, *J. Phys. Chem. B* **104**, 2460 (2000).
- R. Richert, *J. Phys.: Condens. Matter* **14**, R703 (2002).
- W. Kob, C. Donati, S. J. Plimpton, P. H. Poole, and S. C. Glotzer, *Phys. Rev. Lett.* **79**, 2827 (1997).
- C. Donati, J. F. Douglas, W. Kob, S. J. Plimpton, P. H. Poole, and S. C. Glotzer, *Phys. Rev. Lett.* **80**, 2338 (1998).
- C. Donati, S. C. Glotzer, and P. H. Poole, *Phys. Rev. Lett.* **82**, 5064 (1999).
- E. Flenner and G. Szamel, *J. Phys.: Condens. Matter* **19**, 205125 (2007).
- B. Doliwa and A. Heuer, *Phys. Rev. E* **61**, 6898 (2000).
- E. R. Weeks, J. C. Crocker, and D. A. Weitz, *J. Phys.: Condens. Matter* **19**, 205131 (2007).
- N. Lačević, F. W. Starr, T. B. Schröder, and S. C. Glotzer, *J. Chem. Phys.* **119**, 7372 (2003).
- A. S. Keys, A. R. Abate, S. C. Glotzer, and D. J. Durian, *Nat. Phys.* **3**, 260 (2007).
- G. A. Appignanesi, J. A. Rodriguez Fris, R. A. Montani, and W. Kob, *Phys. Rev. Lett.* **96**, 057801 (2006).
- G. A. Appignanesi and J. A. Rodriguez Fris, *J. Phys.: Condens. Matter* **21**, 203103 (2009).
- G. A. Appignanesi, J. A. Rodriguez Fris, and M. A. Frechero, *Phys. Rev. Lett.* **96**, 237803 (2006).
- J. A. Rodriguez Fris, L. M. Alarcón, and G. A. Appignanesi, *Phys. Rev. E* **76**, 011502 (2007).
- J. A. Rodriguez Fris, G. A. Appignanesi, and E. R. Weeks, *Phys. Rev. Lett.* **107**, 065704 (2011).
- C. Toninelli, M. Wyart, L. Berthier, G. Biroli, and J.-P. Bouchaud, *Phys. Rev. E* **71**, 041505 (2005).
- L. Berthier, G. Biroli, J.P. Bouchaud, and R. L. Jack, "Overview of different characterizations of dynamic heterogeneity," in *Dynamical Heterogeneities in Glasses, Colloids, and Granular Media*, edited by L. Berthier, G. Biroli, J.-P. Bouchaud, L. Cipelletti, and W. van Saarloos (Oxford University Press, 2011), ISBN: 9780199691470.
- P. Ball, *Proc. Natl. Acad. Sci. U. S. A.* **114**, 13327 (2017).
- D. M. Huang and D. Chandler, *Proc. Natl. Acad. Sci. U. S. A.* **97**, 8324 (2000).
- X. Huang, C. J. Margulis, and B. J. Berne, *Proc. Natl. Acad. Sci. U. S. A.* **100**, 11953 (2003).
- N. Giovambattista, P. G. Debenedetti, C. F. Lopez, and P. J. Rossky, *Proc. Natl. Acad. Sci. U. S. A.* **105**, 2274 (2008).
- A. Bizzarri and S. Cannistraro, *J. Phys. Chem. B* **106**, 6617 (2002).
- D. Vitkup, D. Ringe, G. A. Petsko, and M. Karplus, *Nat. Struct. Biol.* **7**, 34 (2000).
- N. Choudhury and B. Montgomery Pettitt, *J. Phys. Chem. B* **109**, 6422 (2005).
- H. E. Stanley, P. Kumar, L. Xu, Z. Yan, M. G. Mazza, S. V. Buldyrev, S.-H. Chen, and F. Mallamace, *Physica A* **386**, 729 (2007).
- E. P. Schulz, L. M. Alarcón, and G. A. Appignanesi, *Eur. Phys. J. E* **34**, 114 (2011).
- D. C. Malaspina, E. P. Schulz, L. M. Alarcón, M. A. Frechero, and G. A. Appignanesi, *Eur. Phys. J. E* **32**, 35 (2010).
- L. M. Alarcón, D. C. Malaspina, E. P. Schulz, M. A. Frechero, and G. A. Appignanesi, *Chem. Phys.* **388**, 47 (2011).
- S. R. Accordino, D. C. Malaspina, J. A. Rodriguez Fris, L. M. Alarcón, and G. A. Appignanesi, *Phys. Rev. E* **85**, 031503 (2012).
- S. R. Accordino, J. M. Montes de Oca, J. A. Rodriguez Fris, and G. A. Appignanesi, *J. Chem. Phys.* **143**, 154704 (2015).
- J. M. Montes de Oca, C. A. Menéndez, S. R. Accordino, D. C. Malaspina, and G. A. Appignanesi, *Eur. Phys. J. E* **40**, 78 (2017).
- P. G. Debenedetti, *Metastable Liquids* (Princeton University Press, Princeton, NJ, 1996).
- O. Mishima and H. E. Stanley, *Nature* **396**, 329 (1998).
- C. A. Angell, *Chem. Rev.* **102**, 2627 (2002).
- C. A. Angell, *Annu. Rev. Phys. Chem.* **55**, 559 (2004).
- E. Shiratani and M. Sasai, *J. Chem. Phys.* **104**, 7671 (1996).
- E. Shiratani and M. Sasai, *J. Chem. Phys.* **108**, 3264 (1998).
- M. Sasai, *Physica A* **285**, 315 (2000).
- M. Sasai, *J. Chem. Phys.* **118**, 10651 (2003).
- H. Tanaka, *Phys. Rev. Lett.* **80**, 5750 (1998).
- H. Tanaka, *Europhys. Lett.* **50**, 340 (2000).
- H. Tanaka, *J. Chem. Phys.* **112**, 799 (2000).
- G. A. Appignanesi, J. A. Rodriguez Fris, and F. Sciortino, *Eur. Phys. J. E* **29**, 305 (2009).
- S. R. Accordino, J. A. Rodriguez Fris, F. Sciortino, and G. A. Appignanesi, *Eur. Phys. J. E* **34**, 48 (2011).
- D. C. Malaspina, J. A. Rodriguez Fris, G. A. Appignanesi, and F. Sciortino, *Europhys. Lett.* **88**, 16003 (2009).
- S. R. Accordino, D. C. Malaspina, J. A. Rodriguez Fris, and G. A. Appignanesi, *Phys. Rev. Lett.* **106**, 029801 (2011).
- J. M. Montes de Oca, J. A. Rodriguez Fris, S. R. Accordino, D. C. Malaspina, and G. A. Appignanesi, *Eur. Phys. J. E* **39**, 124 (2016).
- P. Gallo *et al.*, *Chem. Rev.* **116**, 7463 (2016).
- P. H. Handle, T. Loerting, and F. Sciortino, *Proc. Natl. Acad. Sci. U. S. A.* **114**, 13336 (2017).
- P. H. Handle, M. Seidl, and T. Loerting, *Phys. Rev. Lett.* **108**, 225901 (2012).
- K. Amann-Winkel, C. Gainaru, P. H. Handle, M. Seidl, H. Nelson, R. Böhmer, and T. Loerting, *Proc. Natl. Acad. Sci. U. S. A.* **110**, 17720 (2013).
- F. Perakis *et al.*, *Proc. Natl. Acad. Sci. U. S. A.* **114**, 8193 (2017).
- P. H. Handle and T. Loerting, *J. Chem. Phys.* **148**, 124508 (2018).
- P. H. Handle and F. Sciortino, *J. Chem. Phys.* **148**, 134505 (2018).
- J. C. Palmer, P. H. Poole, F. Sciortino, and P. G. Debenedetti, *Chem. Rev.* **118**, 9129–9151 (2018).
- J. L. F. Abascal and C. Vega, *J. Chem. Phys.* **133**, 234502 (2010).
- T. Sumi and H. Sekino, *RSC Adv.* **3**, 12743 (2013).
- R. S. Singh, J. W. Biddle, P. G. Debenedetti, and M. A. Anisimov, *J. Chem. Phys.* **144**, 144504 (2016).
- J. W. Biddle, R. S. Singh, E. M. Sparano, F. Ricci, M. A. Gonzalez, C. Valeriani, J. L. Abascal, P. G. Debenedetti, M. A. Anisimov, and F. Caupin, *J. Chem. Phys.* **146**, 034502 (2017).
- E. La Nave and F. Sciortino, *J. Phys. Chem. B* **108**, 19663 (2004).
- J. A. Rodriguez Fris, G. A. Appignanesi, E. La Nave, and F. Sciortino, *Phys. Rev. E* **75**, 041501 (2007).
- J. A. Rodriguez Fris, E. R. Weeks, F. Sciortino, and G. A. Appignanesi, *Phys. Rev. E* **97**, 060601 (2018).
- K. E. Avila, H. E. Castillo, A. Fiege, K. Vollmayr-Lee, and A. Zippelius, *Phys. Rev. Lett.* **113**, 025701 (2014).

- ⁷⁶S. Chakrabarty, I. Tah, S. Karmakar, and C. Dasgupta, *Phys. Rev. Lett.* **119**, 205502 (2017).
- ⁷⁷W. Kob and H. C. Andersen, *Phys. Rev. E* **51**, 4626 (1995).
- ⁷⁸E. R. Weeks, J. C. Crocker, A. C. Levitt, A. Schofield, and D. A. Weitz, *Science* **287**, 627 (2000).
- ⁷⁹J. L. F. Abascal and C. Vega, *J. Chem. Phys.* **123**, 234505 (2005).
- ⁸⁰C. Vega and J. L. F. Abascal, *Phys. Chem. Chem. Phys.* **13**, 19663 (2011).
- ⁸¹D. Van Der Spoel, E. Lindahl, B. Hess, G. Gerrit, A. E. Mark, E. Alan, and H. J. C. Berendsen, *J. Comput. Chem.* **26**, 1701 (2005).
- ⁸²S. Nosé, *Mol. Phys.* **52**, 255 (1984).
- ⁸³W. G. Hoover, *Phys. Rev. A* **31**, 1695 (1985).
- ⁸⁴U. Essmann, L. Perera, M. L. Berkowitz, T. Darden, H. Lee, and L. G. Pedersen, *J. Chem. Phys.* **103**, 8577 (1995).
- ⁸⁵B. Hess, *J. Chem. Theory Comput.* **4**, 116 (2008).
- ⁸⁶J. Ohmine and H. Tanaka, *Chem. Rev.* **93**, 2545 (1993).
- ⁸⁷C. Liu, Y. Zhang, J. Zhang, J. Wang, W. Li, and W. Wang, *J. Chem. Phys.* **148**, 184502 (2018).
- ⁸⁸J. Qvist, H. Schober, and B. Halle, *J. Chem. Phys.* **134**, 144508 (2011).
- ⁸⁹L. Fabbian, F. Sciortino, and P. Tartaglia, *J. Non-Cryst. Solids* **235-237**, 325 (1998).
- ⁹⁰D. Chandler, in *Introduction to Modern Statistical Mechanics*, edited by D. Chandler (Oxford University Press, 1987), pp. 288.
- ⁹¹P. Gallo and M. Rovere, *J. Chem. Phys.* **137**, 164503 (2012).
- ⁹²P. G. Debenedetti and F. H. Stillinger, *Nature* **410**, 259 (2001).
- ⁹³K. H. Kim *et al.*, *Science* **358**, 1589 (2017).
- ⁹⁴R. Shi, J. Russo, and H. Tanaka, *Proc. Natl. Acad. Sci. U. S. A.* **115**, 9444 (2018).